Available online at www.sciencedirect.com
SCIENCE DIRECT®
International Journal of Heat and Mass Transfer 48 (2005) 119–133
International Journal of HEAT and MASS TRANSFER
www.elsevier.com/locate/ijhmt

Identification methods in nonlinear heat conduction. Part II: inverse problem using a reduced model

Manuel Girault *, Daniel Petit *

Laboratoire d'Etudes Thermiques, UMR n° 6608 du CNRS, ENSMA, Téléport 2, 1 avenue Clément Ader, BP 40109, Futuroscope Cedex 86961, France

Received 16 November 2003; received in revised form 4 May 2004
Available online 17 September 2004

Abstract

A method for solving nonlinear Inverse Heat Conduction Problems (IHCPs) using a Reduced Model (RM) is proposed in this numerical study. In a first step, RM is identified through a specific procedure using optimization techniques and a Detailed Model (DM). Compared to DM, RM allows drastic reduction of computing time without significant loss of accuracy. The second step is the sequential resolution of the inverse problem using RM, taking into account data at *Future Time Steps* in order to estimate a time-varying thermal input from the knowledge of simulated temperature measurements inside the domain. A transient 3D example with thermal conductivity linearly dependant on temperature illustrates the method. It is shown, on this example, that the proposed inversion algorithm using a simple Euler implicit scheme in time gives good results with RM, whereas it does not work with DM.

1. Introduction

Although direct problems consist in the determination of a state variable field, temperature for example, when a mathematical model is available and initial and boundary conditions are known, inverse problems are concerned with the estimation of unknown quantities such as thermophysical properties, initial or boundary conditions, geometric characteristics, from experimental data (temperature or heat fluxes measurements for example).

Inverse methods can be very useful when dealing with industrial systems involving heat transfer in which direct temperature or heat flux measurements are difficult, even impossible, to obtain. Such a situation occurs when the zone of interest is not accessible, or when severe conditions would destroy the sensors. Inverse methods provide tools to estimate unknown quantities from the knowledge of information in another part of the domain. Such inverse problems are often ill-posed, that is: (i) the solution may not exist; (ii) if a solution exists, it can be not unique; (iii) the problem can be unstable. In order to improve the stability of the solution, regularization techniques have been developed by pioneering authors. Let us mention the *Function Specification Method* taking into account information at *Future Time Steps* [1], the *Tikhonov's Regularization Method* [2], the *Iterative Regularization Method* [3], and the *Singular Value Decomposition* (SVD) technique [4].

* Corresponding authors. Tel.: +33 5 49 49 8136; fax: +33 5 49 49 8101 (M. Girault); tel.: +33 5 49 49 8113; fax: +33 5 49 49 8101 (D. Petit).
E-mail addresses: girault@let.ensma.fr (M. Girault), petit@let.ensma.fr (D. Petit).

0017-9310/$ - see front matter © 2004 Elsevier Ltd. All rights reserved.
doi:10.1016/j.ijheatmasstransfer.2004.06.033

Nomenclature

Latin characters

A, B, C, E, F, G, H, P, Q, T, V, X, Y, Z, $\mathbf{C}$, $\mathbf{Y}$	matrices and vectors
C_p	specific heat ($J kg^{-1} K^{-1}$)
DM, RM	Detailed Model, Reduced Model
dimz(n)	$= n(n+1)/2$, n integer
N	DM order i.e. number of discretization nodes
n	RM order
nt	number of time steps
nf	number of *Future Time Steps* (or FTS)
q	output vector dimension
t	time (s)
U	thermal input

Greek symbols

α	under-relaxation parameter
Δt	time step (s)
λ	thermal conductivity ($W m^{-1} K^{-1}$)
ρ	density ($kg m^{-3}$)
Ω, Ψ, Σ	matrix and vectors
σ	standard deviation of noise (°C)
σ_Y	mean quadratic error on temperature data (°C)
σ_U	mean quadratic error on estimates ($W m^{-2}$)

Subscripts

k	time index
s	static

Superscripts

$\bullet$	derivation with respect to time
m	measured
$\hat{}$	estimated
it	iteration index
-1, $-j$	inverse of matrix, power of the inverse

Generally multidimensional Inverse Heat Conduction Problems (IHCPs) require large memory size and computing time induced by large systems of equations associated with the spatial meshing of the domain.

Whole time domain methods using conjugate gradients and an adjoint problem [5–7] have been used to solve 3D IHCPs with unknown boundary conditions. Algorithms and equations for solving nonlinear 3D IHCPs in regular coordinates (rectangular, cylindrical, spherical) by means of the conjugate gradients method and the *Iterative Regularization Method* are given in [7]. Whole time domain approaches offer to use data at all time steps but of course unknowns at all times are estimated together and the cost in terms of computing time can be important.

Sequential methods have also been developed for the resolution of nonlinear IHCPs. They allow faster computations but one may have to deal with larger oscillations of the solution with respect to time. An algorithm using the *Function Specification Method* has been proposed for large variations of thermophysical properties with temperature [8]. For small variations of thermophysical properties, it has been proposed to linearise the problem at each time step of inversion, by assuming constant properties for all *Future Time Steps* [9]. The algorithm is then not iterative in that case. Using the same assumption, a 2D general algorithm, coupling the *Function Specification Method* and the *Tikhonov's Regularization Method*, is proposed in [10]. These two techniques are also coupled in an approach based on Boundary Elements Method (BEM) and Kirchhoff transform for solving multidimensional nonlinear IHCPs [11]. The BEM allows to reduce model size in comparison with classical discretization techniques by limiting the mesh to the boundaries.

When considering transient systems, it is possible to achieve model size reduction by using *reduction methods*. They consist in replacing a classical large size model or Detailed Model (DM) obtained by a spatial discretization of the domain using Finite Elements, Finite Volumes, Finite Differences, etc., and whose order N corresponds to the number of discretization nodes, by a Reduced Model (RM) with $n \ll N$ equations to solve. The use of a RM instead of a DM for solving the inverse problem allows important saves in CPU time [12–15].

The Karhunen-Loève–Galerkin method [16], based on statistical considerations and also known as Proper Orthogonal Decomposition (POD), has been applied to build RMs used for solving nonlinear inverse problems, of conduction [14] as well as of natural convection [15].

The inverse method described in this paper can be applied to multidimensional nonlinear IHCPs, for the estimation of a time-varying boundary condition or internal heat source. It uses a RM which is identified prior to the inverse problem resolution. The identification procedure is detailed in [17]. The inverse algorithm is sequential and *Future Time Steps* coupled with the *Function Specification Method* can be used to improve the quality of estimations. Thanks to the RM small size, computations

are very fast and authorise the use of iterations for the treatment of nonlinearities.

2. Expression of the detailed model

Let us assume a system composed of a purely diffusive medium whose thermal conductivity varies with temperature according to the following law:

$$\lambda(r,T) = \lambda_0(r) + f(r,T) \tag{1}$$

where f is a function of position r and local temperature T and $\lambda_0(r)$ is a conductivity reference distribution.

Density and specific heat are supposed to be invariant with temperature.

Transient energy equation governing heat transfer through the domain is written:

$$\rho(r)C_p(r)\frac{\partial T}{\partial t}(r,t) = \mathrm{div}(\lambda(r,T)\,\vec{\mathrm{grad}}\,T(r,t)) \tag{2}$$

After spatial discretization (using Finite Elements, Finite Volumes, Finite Differences, ...), this equation and the associated boundary conditions can then be written under discrete matrix form known as "*State Space Representation*", forming a DM of the system [17]:

$$\begin{cases} \dot{T}(t) = AT(t) + BU(t) + \Psi(T(t)) \\ Y(t) = CT(t) \end{cases} \tag{3a,b}$$

where $T(t)$ (dim. N) is the vector containing temperatures of all discretization nodes, $\dot{T}(t)$ is the derivative of vector T with respect to time, matrix A (dim. N, N) is the state matrix of a linear system with same geometry but constant thermal conductivity field $\lambda_0(r)$, $\Psi(T(t))$ (dim. N) is the vector gathering nonlinearities effects, hence corresponding to term $f(r, T)$ of Eq. (1). For each node i, component Ψ_i of vector Ψ is the sum of nonlinear contributions of node i with its neighbouring nodes. $U(t)$ is a thermal input (a heat flux density for instance) and vector B (dim. N) is the command or input vector linking nodes to $U(t)$. Matrix C (dim. q, N) with $q = N$ is the observation or output matrix which allows to select a part of the whole temperature field T. This selection is contained in output vector $Y(t)$ (dim. q).

3. Identification of the Reduced Model

3.1. Principle

The reduction method is described in detail in [17] and can be summarised as follows. It derives from the Modal Identification Method [12,13,18] developed for linear systems. Starting from DM structure, RM structure is defined. Elements (matrices) of this RM structure have then to be identified. The identification principle is based on the minimization of a squared residues functional built with the discrepancy between system responses (DM outputs in this paper) on the one hand and RM outputs on the other hand, when a specific input signal is applied. In this study, due to nonlinearities, the reduction method is applied to a mono-input/multi-outputs system.

3.2. Reduced model formulation

From Eqs. (3a,b), it has been shown in [17] that a RM structure can be expressed under the form:

$$\begin{cases} \dot{X}(t) = FX(t) + \underline{\mathbf{1}}U(t) + \Omega Z(X(t)) \\ \hat{Y}(t) = HX(t) \end{cases} \tag{4a,b}$$

where $X(t)$ (dim. n) is a low dimensional state vector ($n \ll N$), $\dot{X}(t)$ its derivative with respect to time. States $X_i(t)$ are coupled through nonlinearities.

$Z(X(t))$ (dim. dimz(n) = $n(n+1)/2$) is the vector of nonlinearities gathering products $X_i(t)X_j(t)$:

$$\begin{aligned} Z(X(t)) = \Big[& X_1^2(t) \quad X_1(t)X_2(t) \quad X_1(t)X_3(t) \quad \cdots \\ & X_1(t)X_n(t) \quad X_2^2(t) \quad X_2(t)X_3(t) \quad \cdots \\ & X_2(t)X_n(t) \quad \cdots \quad \cdots \quad X_{n-1}^2(t) \\ & X_{n-1}(t)X_n(t) \quad X_n^2(t) \Big]^{\mathrm{T}} \end{aligned} \tag{5}$$

where $\underline{\mathbf{1}}$ is the vector whose dimension is n and all components are equal to 1, $U(t)$ is the thermal input, and $\hat{Y}(t)$ (dim. q) is the approached output vector (such as $\hat{Y}(t) \approx Y(t)$).

F (dim. n, n) is a diagonal matrix containing n characteristic "eigenvalues" to be *identified*. Ω (dim. n, dimz(n)) is the matrix quantifying the contribution of components of nonlinear vector $Z(X(t))$ in each one of the n coupled equations. Components of Ω have to be *identified*. H (dim. q, n) is a reduced output matrix which has to be *identified*.

3.3. Reduced model identification algorithm

The identification of components of matrices F, Ω and H is realised through the minimization of a squared residues functional J_{red} built with the discrepancy between responses of the system (in this study, outputs of DM defined by Eqs. (3a,b)) on the one hand and outputs of RM defined by Eqs. (4a,b) on the other hand, when a specific input signal is applied [17]:

$$J_{\mathrm{red}}(n,F,\Omega,H) = \sum_{i=1}^{q}\sum_{j=0}^{\mathrm{nt}}(Y_i(t_j) - \hat{Y}_i(t_j))^2 \tag{6}$$

where 'nt' is the number of time steps in the simulations and the t_j are the discretization times.

Quadratic criterion J_{red} depends on RM order n. Starting with $n = 1$, n is incremented and a RM is identified for each value of n until the gap between two successive criterions is very low or until the discrepancy between RM and DM's responses is of the order of magnitude of the precision wanted by the user.

The minimization algorithm uses *linear least squares* coupled to a *Quasi-Newton* type method.

4. Resolution of the inverse problem using DM and RM

In this part is presented the inversion algorithm developed to estimate an unknown boundary condition $U(t)$ from the knowledge of temperature data $Y(t)$, when the system is modelled with a DM (Eqs. (3a,b)) or a RM (Eqs. (4a,b)). The procedure is sequential in time and *Future Time Steps* can be used to take into account lagging and damping effects due to heat diffusion [1,9,10,19], as well as to regularize the inverse problem.

4.1. Common state space representation for DM and RM

Both DM (Eqs. (3a,b)) and RM (Eqs. (4a,b)) can be written under the following general form:

$$\begin{cases} \dot{V} = EV + PU + \Sigma(V) \\ Y = QV \end{cases} \tag{7a,b}$$

$$\text{for DM}: \begin{cases} V = T(\text{dim. } N) \\ E = A(\text{dim. } N, N) \\ P = B(\text{dim. } N) \\ \Sigma(V) = \Psi(T)(\text{dim. } N) \\ Q = C(\text{dim. } q, N) \end{cases} \quad \text{and}$$

$$\text{for RM}: \begin{cases} V = X(\text{dim. } n \ll N) \\ E = F(\text{dim. } n, n) \textit{diagonal} \\ P = \underline{\mathbf{1}}(\text{dim. } n) \\ \Sigma(V) = \Omega Z(X)(\text{dim. } n) \\ Q = H(\text{dim. } q, n) \end{cases}$$

4.2. Resolution of the steady regime

Knowing the steady data Y_s, one searches $\hat{U}_s$. Eqs. (7a,b) in steady regime are written:

$$\begin{cases} 0 = EV_s + PU_s + \Sigma(V_s) \\ Y_s = QV_s \end{cases} \tag{8a,b}$$

As the problem is nonlinear, an initial guess is needed. A good first approximation is $\hat{U}_s^{\text{it}=0} = \hat{U}_s^{\text{lin}}$, solution of the inverse problem with the steady state linear model obtained by zeroing the nonlinear term $\Sigma(V_s)$ in Eq. (8a). From this model one gets: $\mathbf{C}U_s = \mathbf{Y}$ with $\mathbf{C} = -QE^{-1}P$ and $\mathbf{Y} = Y_s$.

The solution given by linear least squares is $\hat{U}_s^{\text{it}=0} = \hat{U}_s^{\text{lin}} = (\mathbf{C}^{\mathrm{T}}\mathbf{C})^{-1}\mathbf{C}^{\mathrm{T}}\mathbf{Y}$.

The initial guess for the state vector V_s is then written: $\hat{V}_s^{\text{it}=0} = \hat{V}_s^{\text{lin}} = -E^{-1}P\hat{U}_s^{\text{lin}}$.

From Eqs. (8a,b), one can write: $-QE^{-1}PU_s = Y_s + QE^{-1}\Sigma(V_s)$.

Iterations are thus performed on the following equation:

$$\hat{U}_s^{\text{it}+1} = (\mathbf{C}^{\mathrm{T}}\mathbf{C})^{-1}\mathbf{C}^{\mathrm{T}}\mathbf{Y}^{\text{it}} \tag{9}$$

with

$$\mathbf{C} = -QE^{-1}P \tag{10}$$

and

$$\mathbf{Y}^{\text{it}} = Y_s + QE^{-1}\Sigma(\hat{V}_s^{\text{it}}) \tag{11}$$

where $\hat{V}_s^{\text{it}}$ is the estimation of V_s at iteration 'it'. Then $\hat{V}_s^{\text{it}+1} = -E^{-1}(P\hat{U}_s^{\text{it}+1} + \Sigma(\hat{V}_s^{\text{it}}))$.

This sequence is performed until convergence is obtained i.e.: $\hat{U}_s^{\text{it}+1} \cong \hat{U}_s^{\text{it}}$. The estimated output vector can be computed using state vector $\hat{V}_s^{\text{cv}}$ estimated after convergence: $\hat{Y}_s = Q\hat{V}_s^{\text{cv}}$.

The proposed method allows to estimate a thermal input in steady state from one or more temperature data.

4.3. Resolution of the transient regime

The previous method also permits to initialise an identification in transient regime by using for the first time step:

$$\hat{V}_0 = \hat{V}_s^{\text{cv}} \quad \text{and} \quad \hat{U}_0 = \hat{U}_s^{\text{cv}}$$

Knowing Y_{k+1} at time step $k + 1$ and $\hat{V}_k$ at time step k, one searches $\hat{U}_{k+1}$.

Starting with $\hat{V}_{k+1}^{\text{it}=0} = \hat{V}_k$ as initial guess for the time step, iterations on the solution of Eqs. (7a,b) are performed: from Eq. (7a), one can write, with Δt the time step and an Euler implicit scheme:

$$\dot{V} = \frac{V_{k+1} - V_k}{\Delta t} = EV_{k+1} + PU_{k+1} + \Sigma(V_{k+1})$$

Then

$$V_{k+1} = (I - E\Delta t)^{-1}[V_k + P\Delta t U_{k+1} + \Sigma(V_{k+1})\Delta t] \tag{12}$$

Hence, according to Eq. (7b):

$$Y_{k+1} = Q(I - E\Delta t)^{-1}[V_k + P\Delta t U_{k+1} + \Sigma(V_{k+1})\Delta t] \tag{13}$$

which can also be written: $\mathbf{C}U_{k+1} = \mathbf{Y}$ with

$$\mathbf{C} = Q(I - E\Delta t)^{-1}P\Delta t \tag{14}$$

and $\mathbf{Y} = Y_{k+1} - Q(I - E\Delta t)^{-1}[V_k + \Sigma(V_{k+1})\Delta t]$.

The solution given by linear least squares is $\hat{U}_{k+1} = (\mathbf{C}^{\mathrm{T}}\mathbf{C})^{-1}\mathbf{C}^{\mathrm{T}}\mathbf{Y}$.

Iterations are thus performed on the following equation:

$$\hat{U}_{k+1}^{\mathrm{it}+1} = (\mathbf{C}^{\mathrm{T}}\mathbf{C})^{-1}\mathbf{C}^{\mathrm{T}}\mathbf{Y}^{\mathrm{it}} \tag{15}$$

with

$$\mathbf{Y}^{\mathrm{it}} = Y_{k+1} - Q(I - E\Delta t)^{-1}[\hat{V}_k + \Sigma(\hat{V}_{k+1}^{\mathrm{it}})\Delta t] \tag{16}$$

where $\hat{V}_k$ is the estimation of V_k and $\hat{V}_{k+1}^{\mathrm{it}}$ is the estimation of V_{k+1} at iteration *it*. Then

$$\hat{V}_{k+1}^{\mathrm{it}+1} = (I - E\Delta t)^{-1}[\hat{V}_k + P\Delta t\hat{U}_{k+1}^{\mathrm{it}+1} + \Sigma(\hat{V}_{k+1}^{\mathrm{it}})\Delta t]$$

This sequence is performed until convergence is obtained i.e.: $\hat{U}_{k+1}^{\mathrm{it}+1} \cong \hat{U}_{k+1}^{\mathrm{it}}$. The estimated output vector is can be computed using state vector $\hat{V}_{k+1}^{\mathrm{cv}}$ estimated after convergence: $\hat{Y}_{k+1} = Q\hat{V}_{k+1}^{\mathrm{cv}}$.

4.3.1. Introduction of Future Time Steps (FTS):

Let us use data at ***nf*** *Future Time Steps* $k+2, k+3, k+1+f, \ldots, k+1+$ ***nf*** ($f = 1, 2, \ldots,$ ***nf***). The *Function Specification Method* [1,9,10,12,13,19] is used to make an hypothesis for the unknown input at the ***nf*** *FTS*:

$$U_{k+1+f} = U_{k+1} = \text{constant}, \quad f \in [1, \boldsymbol{nf}\,] \tag{17}$$

Remark. The way to choose the number ***nf*** of Future Time Steps is explained at the beginning of Section 6.3 (example of application).

For f = 1. Eq. (13) written for $Y_{k+2} = Y_{k+1+1}$ leads to

$$Y_{k+2} = Q(I - E\Delta t)^{-1}[V_{k+1} + P\Delta tU_{k+2} + \Sigma(V_{k+2})\Delta t]$$

Injecting Eq. (12), one obtains

$$Y_{k+2} = Q(I - E\Delta t)^{-1}\Big[(I - E\Delta t)^{-1}[V_k + P\Delta tU_{k+1} + \Sigma(V_{k+1})\Delta t] + P\Delta tU_{k+2} + \Sigma(V_{k+2})\Delta t\Big]$$

which can also be written:

$$Y_{k+2} = Q(I - E\Delta t)^{-2}[V_k + P\Delta tU_{k+1} + \Sigma(V_{k+1})\Delta t] + Q(I - E\Delta t)^{-1}[P\Delta tU_{k+2} + \Sigma(V_{k+2})\Delta t]$$

According to hypothesis (17), one has

$$Y_{k+2} = Q(I - E\Delta t)^{-2}[V_k + \Sigma(V_{k+1})\Delta t] + Q(I - E\Delta t)^{-1}\Sigma(V_{k+2})\Delta t + Q[(I - E\Delta t)^{-1} + (I - E\Delta t)^{-2}]P\Delta tU_{k+1}$$

which can be rewritten:

$$Q\lfloor(I - E\Delta t)^{-1} + (I - E\Delta t)^{-2}\rfloor P\Delta tU_{k+1} = Y_{k+2} - Q(I - E\Delta t)^{-2}[V_k + \Sigma(V_{k+1})\Delta t] - Q(I - E\Delta t)^{-1}\Sigma(V_{k+2})\Delta t$$

For a current value f, it can be shown that using Eqs. (12), (13) *and* (17).

$$Y_{k+1+f} = Q(I - E\Delta t)^{-(f+1)}[V_k + \Sigma(V_{k+1})\Delta t] + \sum_{j=1}^{f} Q(I - E\Delta t)^{-j}\Sigma(V_{k+1+f-j+1})\Delta t + Q\left[\sum_{j=1}^{f+1}(I - E\Delta t)^{-j}\right]P\Delta tU_{k+1}$$

which can also be written:

$$Q\left[\sum_{j=1}^{f+1}(I - E\Delta t)^{-j}\right]P\Delta tU_{k+1} = Y_{k+1+f} - Q(I - E\Delta t)^{-(f+1)}[V_k + \Sigma(V_{k+1})\Delta t] - \sum_{j=1}^{f} Q(I - E\Delta t)^{-j}\Sigma(V_{k+1+f-j+1})\Delta t \tag{18}$$

The ***nf*** equations (18) ($f = 1, 2, \ldots,$ ***nf***) can be written using estimated state vectors, and then gathered in a global matrix form:

$$\mathbf{C}U_{k+1}^{\mathrm{it}+1} = \mathbf{Y}^{\mathrm{it}} \quad (\mathbf{C}\,\text{dim. } (q \times (\boldsymbol{nf}+1), 1), \mathbf{Y}^{\mathrm{it}}\,\text{dim. } q \times (\boldsymbol{nf}+1))$$

Iterations are thus performed on the linear least squares solution:

$$\hat{U}_{k+1}^{\mathrm{it}+1} = (\mathbf{C}^{\mathrm{T}}\mathbf{C})^{-1}\mathbf{C}^{\mathrm{T}}\mathbf{Y}^{\mathrm{it}} \tag{19}$$

with

$$\mathbf{C} = \begin{bmatrix} Q(I - E\Delta t)^{-1}P\Delta t \\ Q[(I - E\Delta t)^{-1} + (I - E\Delta t)^{-2}]P\Delta t \\ Q[(I - E\Delta t)^{-1} + (I - E\Delta t)^{-2} + (I - E\Delta t)^{-3}]P\Delta t \\ \vdots \\ Q\left[\sum_{j=1}^{f+1}(I - E\Delta t)^{-j}\right]P\Delta t \\ \vdots \\ Q\left[\sum_{j=1}^{\boldsymbol{nf}+1}(I - E\Delta t)^{-j}\right]P\Delta t \end{bmatrix} \tag{20}$$

and

$$Y^{\mathrm{it}} = \begin{bmatrix} Y_{k+1} - Q(I-E\Delta t)^{-1}[\hat{V}_k + \Sigma(\hat{V}^{\mathrm{it}}_{k+1})\Delta t] \\ Y_{k+2} - Q(I-E\Delta t)^{-2}[\hat{V}_k + \Sigma(\hat{V}^{\mathrm{it}}_{k+1})\Delta t] - Q(I-E\Delta t)^{-1}\Sigma(\hat{V}^{\mathrm{it}}_{k+2})\Delta t \\ Y_{k+3} - Q(I-E\Delta t)^{-3}[\hat{V}_k + \Sigma(\hat{V}^{\mathrm{it}}_{k+1})\Delta t] - Q(I-E\Delta t)^{-2}\Sigma(\hat{V}^{\mathrm{it}}_{k+2})\Delta t - Q(I-E\Delta t)^{-1}\Sigma(\hat{V}^{\mathrm{it}}_{k+3})\Delta t \\ \vdots \\ Y_{k+1+f} - Q(I-E\Delta t)^{-(f+1)}[\hat{V}_k + \Sigma(\hat{V}^{\mathrm{it}}_{k+1})\Delta t] - \sum_{j=1}^{f} Q(I-E\Delta t)^{-j}\Sigma(\hat{V}^{\mathrm{it}}_{k+1+f-j+1})\Delta t \\ \vdots \\ Y_{k+1+\boldsymbol{nf}} - Q(I-E\Delta t)^{-(\boldsymbol{nf}+1)}[\hat{V}_k + \Sigma(\hat{V}^{\mathrm{it}}_{k+1})\Delta t] - \sum_{j=1}^{\boldsymbol{nf}} Q(I-E\Delta t)^{-j}\Sigma(\hat{V}^{\mathrm{it}}_{k+1+nf-j+1})\Delta t \end{bmatrix} \quad (21)$$

After $\hat{U}^{\mathrm{it}+1}_{k+1}$ is obtained, the $\hat{V}^{\mathrm{it}+1}_{k+1+f}$, $0 \leqslant f \leqslant \boldsymbol{nf}$ are computed successively, using

$$\hat{V}^{\mathrm{it}+1}_{k+1+f} = (I-E\Delta t)^{-1}\left[\hat{V}^{\mathrm{it}+1}_{k+f} + P\Delta t\hat{U}^{\mathrm{it}+1}_{k+1+f} + \Sigma(\hat{V}^{\mathrm{it}}_{k+1+f})\Delta t\right]$$

which is written, according to hypothesis (17):

$$\hat{V}^{\mathrm{it}+1}_{k+1+f} = (I-E\Delta t)^{-1}\left[\hat{V}^{\mathrm{it}+1}_{k+f} + P\Delta t\hat{U}^{\mathrm{it}+1}_{k+1} + \Sigma(\hat{V}^{\mathrm{it}}_{k+1+f})\Delta t\right]$$

One starts with $f = 0$ with: $\hat{V}^{\mathrm{it}+1}_{k} = \hat{V}_k \ \forall \mathrm{it}$.

Values $\Sigma(\hat{V}^{\mathrm{it}=0}_{k+1+f})$, $0 \leqslant f \leqslant \boldsymbol{nf}$, are those computed after convergence in the previous time step of inversion, i.e. the $\Sigma(\hat{V}^{\mathrm{cv}}_{k+f})$. For the first time step of inversion, $\Sigma(\hat{V}^{\mathrm{cv}}_{s})$ computed after convergence in the initial steady state, is taken as initial value for the $\Sigma(\hat{V}^{\mathrm{it}=0}_{k+1+f})$, $0 \leqslant f \leqslant \boldsymbol{nf}$.

4.4. Remarks

- Future Time Steps are not only taking into account lagging and damping effects, but also regularize the inverse problem because it becomes overdetermined as soon as $\boldsymbol{nf} > 0$ ($\boldsymbol{nf} = 0$ corresponds to "no FTS" and only $T(k+1)$ is used to estimate $U(k+1)$, $\boldsymbol{nf} = 1$ corresponds to the use of one future temperature $T(k+2)$ in addition to $T(k+1)$, etc.).
- At each time step, a single unknown is estimated, thus the matrix $\mathbf{C}^{\mathrm{T}}\mathbf{C}$ of the linear system to be solved (Eq. (9), Eq. (15) or Eq. (19)) is a simple scalar, whatever the number of sensors and the number of *Future Time Steps*. The condition number of $\mathbf{C}^{\mathrm{T}}\mathbf{C}$ is therefore equal to 1 at each time step. The inverse problem has then the best possible conditioning. As a consequence, for the sequential resolution of the considered inverse problem, no additional regularization such as Tikhonov's regularization is necessary to solve the linear system at each iteration of each time step. In contrast, it would be useful if a whole time domain method was used or in the case of the estimation of more than one independent unknown.

5. Comments on the use of RM for solving inverse problems

Although at each iteration of each time step, the size of the system solved by linear least squares only depends on the number of unknowns (limited to one in this study), either with RM and DM, the computation with RM is faster and easier than with DM.

The first advantage of RM is of course the smaller size of the state vector V : although for both models, a system of coupled nonlinear partial differential equations of the first order in time has to be solved to obtain the state vector, with DM one has to compute the whole temperature field T (dim. N) at each iteration of each time step, whereas the use of a RM only requires the computation of the reduced state vector X (dim. $n \ll N$) (cf. Eqs. (11), (16) and (21)).

Moreover, the fact that F is diagonal is a great advantage of the RM. This is underlined in Table 1 summarizing the matrices to compute for the inverse problem resolution, according to the model used.

When using a RM, only inverses of diagonal matrices F and $(I - F\Delta t)$ have to be computed. These matrices are therefore easy to obtain. Furthermore, they have only $n \ll N$ components.

Conversely, in the DM case, it can be very difficult, indeed even impossible, to compute inverses of matrices A and $(I - A\Delta t)$ whose dimension is (N, N), especially for large values of N.

That huge advantage is emphasised when *Future Time Steps* are used, since the computation of powers of the diagonal matrix $(I - F\Delta t)^{-1}$ is much more easier than the computation of powers of $(I - A\Delta t)^{-1}$.

Of course, the computation of $A^{-1}(I - A\Delta t)^{-1}$ and its powers can be made prior to the inverse problem resolution. It is nevertheless a laborious operation and even if it is possible, the storage of these matrices may require large memory size.

Table 1
Matrices to compute for solving the inverse problem with each model

	Steady regime (Eqs. (9)–(11))	Transient regime (without FTS) (Eqs. (14)–(16))	Transient regime (with ***nf*** FTS) (Eqs. (19)–(21))
Detailed model	A^{-1}	$(I - A\Delta t)^{-1}$	$(I - A\Delta t)^{-j}$, $j = 1$ to $\boldsymbol{nf} + 1$
Reduced model (F diagonal matrix)	F^{-1}	$(I - F\Delta t)^{-1}$	$(I - F\Delta t)^{-j}$, $j = 1$ to $\boldsymbol{nf} + 1$

6. An example of application

A numerical example is presented to test the proposed inverse algorithm. The case considered in [17] to illustrate the RM identification method is taken. This is a 3D system shown on Fig. 1: a cube (0.1 m × 0.1 m × 0.1 m) composed of a material whose thermal conductivity depends linearly on temperature according to the following law:

$$\lambda(T) = 16(1 + 0.01(T - 20)) \tag{22}$$

where the local temperature T is expressed in °C.

Eq. (2) is considered, with $T = T(x, y, z, t)$ and $\rho C_p = 4.02910^6\ \mathrm{J\,m^{-3}\,°C^{-1}}$.

Associated boundary conditions are written:

$$-\lambda(T)\frac{\partial T}{\partial x} = U(t) \quad \text{at } x = 0 \tag{23a}$$

$$-\lambda(T)\frac{\partial T}{\partial x} = h(T - T_a) \quad \text{at } x = 0.1 \tag{23b}$$

$$T = 0 \quad \text{at } y = 0 \tag{23c}$$

$$\lambda(T)\frac{\partial T}{\partial y} = 0 \quad \text{at } y = 0.1 \tag{23d}$$

$$\lambda(T)\frac{\partial T}{\partial z} = h(T - T_a) \quad \text{at } z = 0 \tag{23e}$$

$$\lambda(T)\frac{\partial T}{\partial z} = 0 \quad \text{at } z = 0.1 \tag{23f}$$

where $T_a = 0\,°C$ is the ambient temperature surrounding east and bottom faces, and $h = 50\,\mathrm{W\,m^{-2}\,°C^{-1}}$ is a convective exchange coefficient.

A possible initial condition is given by the resolution of Eq. (2) in steady state when boundary conditions (23a–f) are applied with $U(t = 0)$.

The domain is discretised using the Finite Volumes Method, with 11 nodes in each direction. In that way, a DM of order $N = 1331$, taking the form of Eqs. (3a,b), is built.

The inverse problem we consider is relative to the estimation of the applied heat flux density $U(t)$ from the knowledge of temperature measurements (simulated in the present paper) inside the domain.

Remark concerning the location of thermosensors and the RM's outputs: in a practical application, the location of sensors is chosen (after sensitivity study and taking into account technical constraints) and then the RM is identified for these points specifically. In the present paper, RM is built in Part I because the objective is to

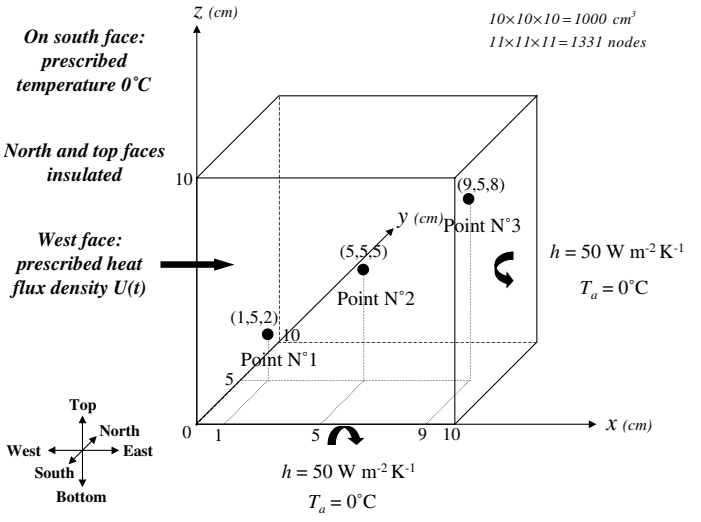

Fig. 1. System description.

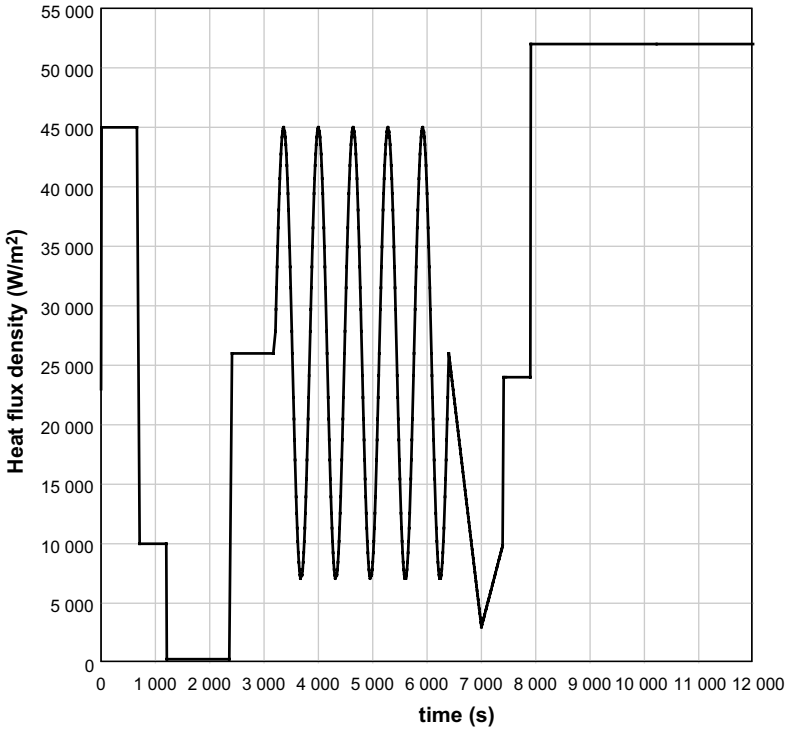

Fig. 2. Test function for $U(t)$.

expose the reduction method, and it is then used in Part II for solving an inverse problem with sensors located at the points for which RM has been built.

Three locations corresponding to RM's outputs of Part I are therefore considered for sensors positions (cf. Fig. 1): the first one near the bottom face and the west face submitted to the boundary condition $U(t)$, the second one at the centre of the cube and the third one near the top face and the east face opposed to the heated boundary. In Part I of the paper [17], five RMs of respective order $n = 1$ to 5, describing the thermal behaviour of these three points, have been identified. The RM of order 4 has been validated by comparing solutions of the direct problem with those obtained using DM, when two different input signals $U(t)$ are applied. A reduction of computing time by a factor greater than 1000 has been observed, without significant loss of accuracy.

It is proposed here to use this identified RM for solving the inverse problem. The function $U(t)$ used to test the inverse algorithm is shown on Fig. 2.

Note: of course, RM has been identified using a different input.

Using Fig. 2 input, temperature evolutions at points 1–3 (cf. Fig. 1) have been computed by solving the direct problem using DM. nt = 1200 time steps, each one of $\Delta t = 10$ s, are considered. The inversion test consists in retrieving $U(t)$ from these temperature data, on the one hand with DM and on the other hand with RM. In a first step, the estimation is performed using "exact temperatures" given by DM. In a second step, a random gaussian noise is added to "exact data" to simulate real measurements. For a discrete temperature evolution T containing the initial temperature and nt time steps, one has

$$T_i = T_i^{\text{exact}} + \omega_i \sigma = T_i^{\text{exact}} + \Delta T_i \quad \forall i \in [0, \text{nt}]$$

where σ is the dimensional standard deviation of measurement errors which is assumed to be the same for all measurements and $\{\omega_i\}$ is a random gaussian distribution of mean value 0 and variance 1. That means there is a 99% probability of the value for ω_i to be in the range $-2.576 < \omega_i < +2.576$, hence $\sigma = 0.5\,\text{K}$ corresponds to errors on temperatures ΔT_i such as $1.3\,\text{K} < \Delta T_i < +1.3\,\text{K}$.

Simulated temperature measurements corresponding to $\sigma = 0.5\,\text{K}$ are shown in Fig. 3.

6.1. The different inversion cases

Four configurations have been studied, on the one hand with unperturbed data ($\sigma = 0\,°\text{C}$) and on the other hand with noisy data ($\sigma = 0.5\,°\text{C}$):

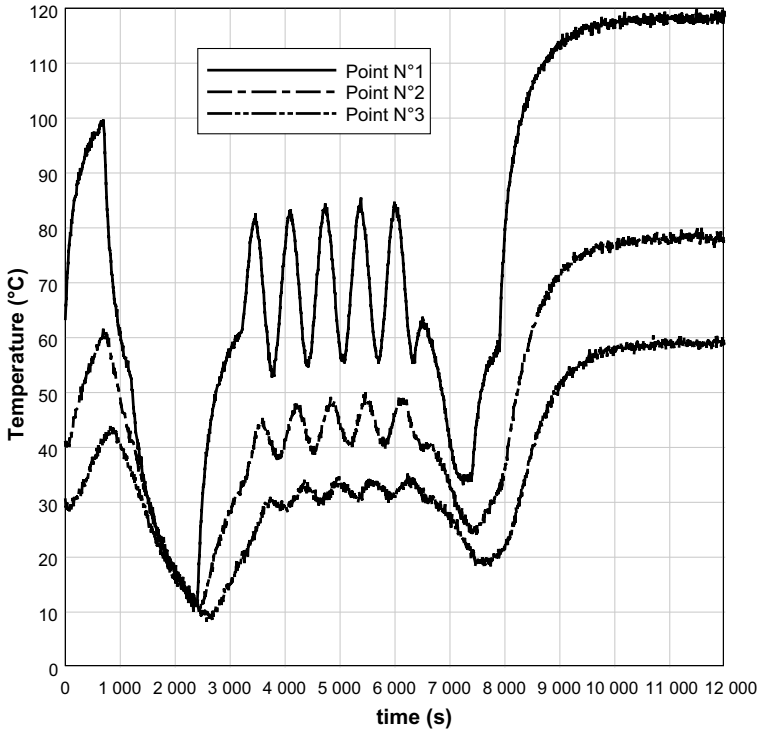

Fig. 3. Simulated temperature measurements.

- A single sensor at point no. 1.
- A single sensor at point no. 2.
- A single sensor at point no. 3.
- The three sensors altogether.

Let us introduce two quantities to evaluate the quality of estimations:

- the mean quadratic error on temperatures σ_Y between $Y^m(t)$ and $\hat{Y}(t)$, where Y^m is the vector of temperature data and $\hat{Y}$ is the vector of the temperatures calculated with the identified inputs:

$$\sigma_Y = \left[\frac{1}{q(\mathrm{nt} - \boldsymbol{nf} + 1)} \sum_{i=1}^{q} \sum_{j=0}^{\mathrm{nt}-\boldsymbol{nf}} (\hat{Y}_i(t_j) - Y_i^m(t_j))^2\right]^{1/2} \tag{24}$$

- the mean quadratic error on estimated inputs σ_U between $U^{\mathrm{exact}}(t)$ and $\hat{U}(t)$, where U^{exact} is the exact input vector and $\hat{U}$ is the vector of the estimated inputs obtained by inversion:

$$\sigma_U = \left[\frac{1}{(\mathrm{nt} - \boldsymbol{nf} + 1)} \sum_{j=0}^{\mathrm{nt}-\boldsymbol{nf}} (\hat{U}_i(t_j) - U_i^{\mathrm{exact}}(t_j))^2\right]^{1/2} \tag{25}$$

The lower σ_U is, the better the inversion is. In the present numerical study, the test input $U^{\mathrm{exact}}(t)$ is available. In real cases, σ_U is unknown unless measurements of U can be made with another method for validation. σ_Y is therefore the only available quantity in practical applications.

6.2. Inversion using DM

It has not been possible to find a solution for the inverse problem using DM *and* the simple Euler implicit scheme used for time integration in the inversion algorithm described in Section 4.1. Nevertheless, it is highly probable, not to say sure, that a solution can be obtained with DM combined with a more advanced time integration scheme.

With the simple algorithm described in Section 4.1, it has not been possible to ensure the convergence when DM is used, even with *Future Time Steps* and/or limitation of the number of iterations at each time step, and whatever the data employed. In supplement, an underrelaxation method of the solution has been used: at each iteration it + 1 of each time step $k + 1$, the following sequence is used after the resolution by the linear least squares method:

$$U_{k+1}^{it+1} \leftarrow \alpha U_{k+1}^{it+1} + (1-\alpha) U_{k+1}^{it} \quad (26)$$

where α is the under-relaxation parameter ($0 < \alpha < 1$).

Whatever the value of α, convergence has not been obtained.

It should be underlined that a solution can be found using RM *and* the same algorithm with a simple Euler implicit scheme. Therefore it appears possible to use RM along with a rather coarse inversion algorithm, which seems not to be the case with DM. A possible (and probable) explanation of that apparently strange fact lies in the own nature of RM: RM is by essence slightly less precise than DM because it does not contain the whole information included in DM: in fact RM's small size (a few equations and a few elements) does not authorize it to reproduce exactly DM's dynamics. But its limited number of degrees of freedom allows it to be less sensitive to round-off errors and, generally speaking, more robust than DM.

6.3. Inversion using RM

For all configurations except the case of sensor at point no. 1 and unperturbed data ($\sigma = 0\,°C$), it has been necessary to use *Future Time Steps* to take into account the lagging and damping effects of heat diffusion, as well as to regularize the inverse problem. When using noisy data, the number ***nf*** of FTS has been determined so that it satisfies the *discrepancy principle*, stipulating that σ_Y should be close to the standard deviation of noise σ [2,19]:

$$\sigma_Y \approx \sigma \quad (27)$$

When using unperturbed data ($\sigma = 0\,°C$), ***nf*** has been increased until oscillations disappear in the estimated signal.

Figs. 4, 6 and 8 respectively show the estimation obtained using unperturbed data of a single sensor at point nos. 1, 2 and 3, although Figs. 5, 7 and 9 respectively show the estimation obtained using noisy data of a single sensor at point nos. 1, 2 and 3. Inversion results using RM are also summarised in Table 2, including the estimation using the three sensors together. Only an order of magnitude of the computing time is given, because it depends on the number of iterations at each time step and on a possible under-relaxation parameter. Of course computing time increases with the number ***nf*** of FTS.

The further of the heated boundary the sensor is located, the more its response is lagged and damped in comparison with the input, and the more sensitive to measurement errors ii becomes. The inversion is therefore more difficult. A dimensionless time step Δt_i characteristic of the inversion feasibility can be defined as [20]:

$$\Delta t_i = \frac{a\Delta t}{e^2} \quad (28)$$

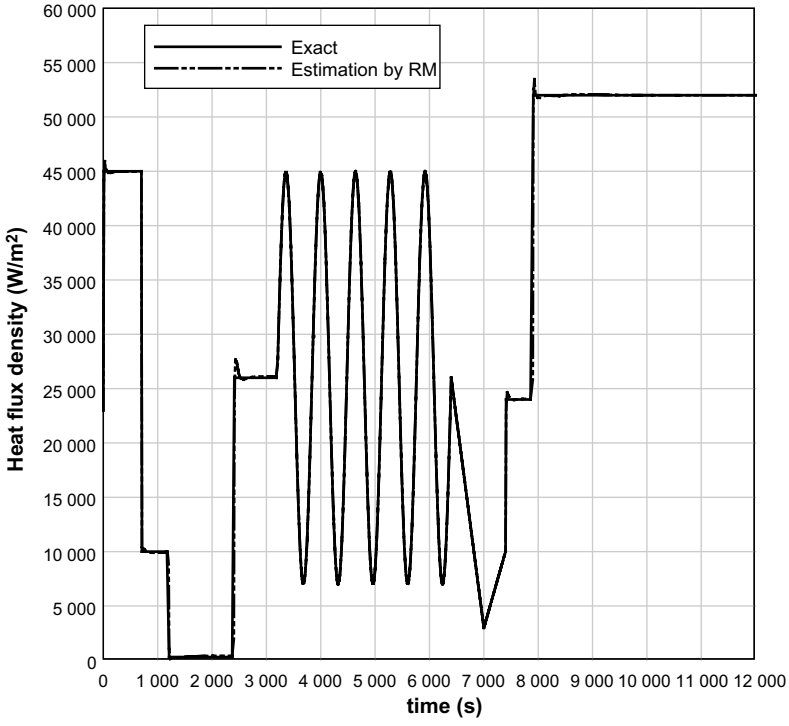

Fig. 4. Estimation using sensor no. 1 with "exact data" ($\sigma = 0\,°C$) and ***nf*** = 1.

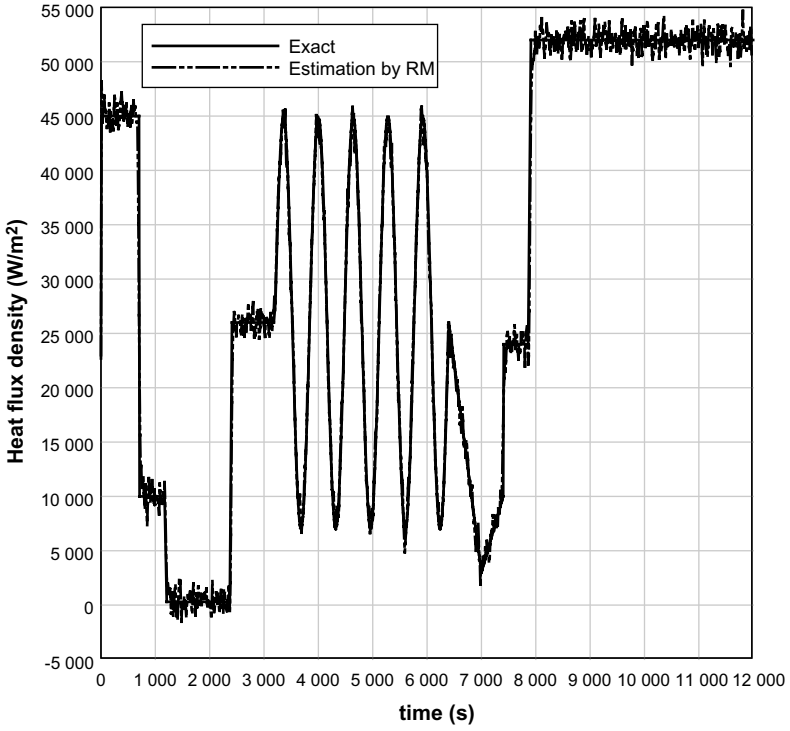

Fig. 5. Estimation using sensor no. 1 with noisy data ($\sigma = 0.5\,^{\circ}\mathrm{C}$) and $nf = 3$.

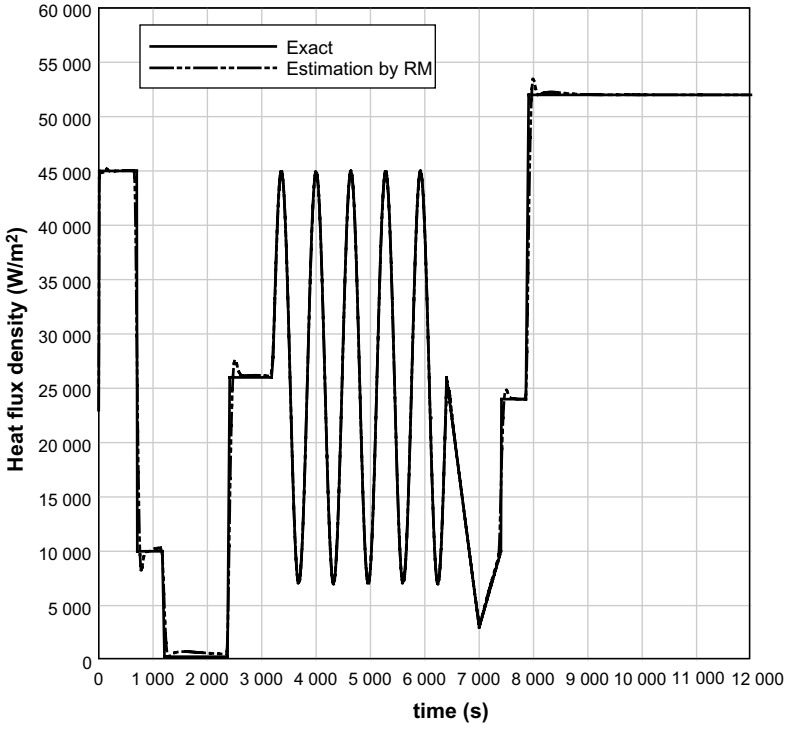

Fig. 6. Estimation using sensor no. 2 with "exact data" ($\sigma = 0\,^{\circ}\mathrm{C}$) and $nf = 10$.

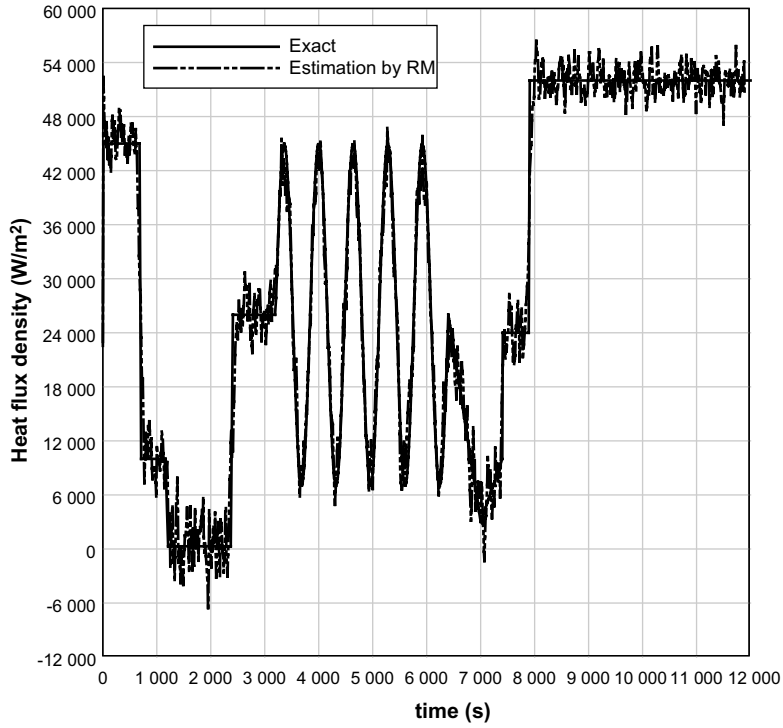

Fig. 7. Estimation using sensor no. 2 with noisy data ($\sigma = 0.5\,^{\circ}\mathrm{C}$) and $nf = 12$.

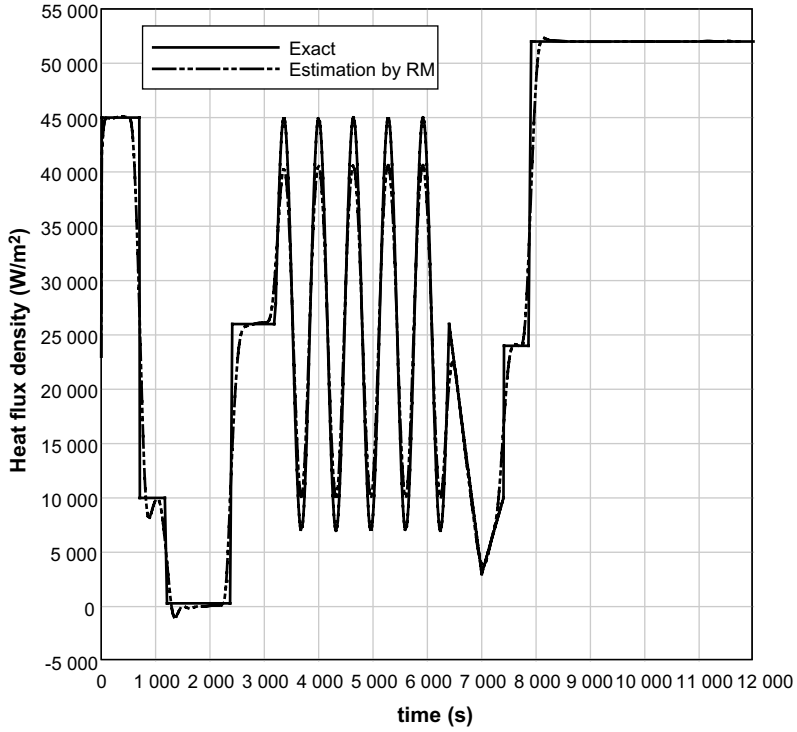

Fig. 8. Estimation using sensor no. 3 with "exact data" ($\sigma = 0\,^{\circ}\mathrm{C}$) and $nf = 26$.

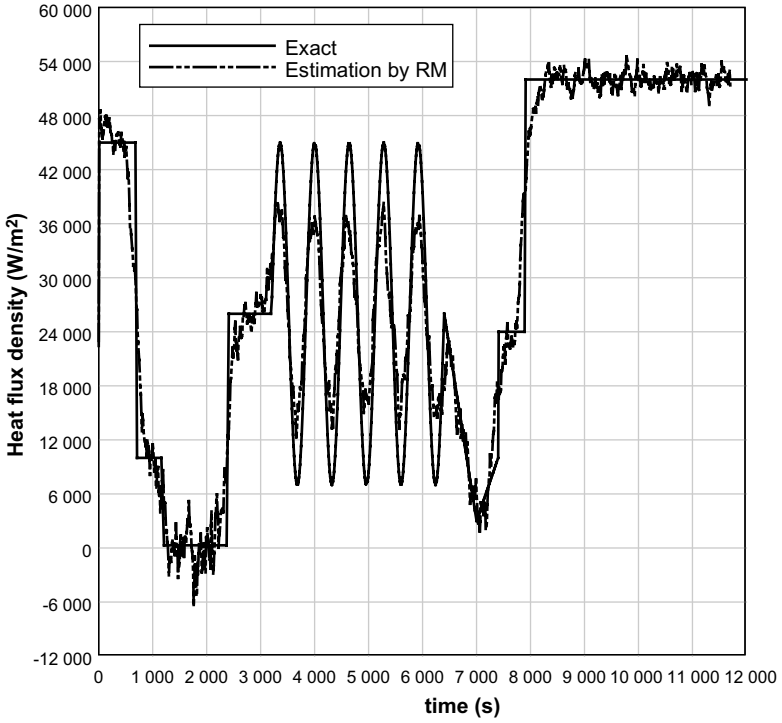

Fig. 9. Estimation using sensor no. 3 with noisy data ($\sigma = 0.5\,°C$) and $\boldsymbol{nf} = 26$.

Table 2
Inversion results for different cases using RM of order 4

Standard deviation of noise	Number of sensors and positions	σ_Y (°C)	σ_U ($W m^{-2}$)	Number ***nf*** of *Future Time Steps*	Order of magnitude of CPU time (s)
$\sigma = 0\,°C$	1 (point no. 1), Fig. 4	9.75×10^{-15}	195	0	0.37
	1 (point no. 2), Fig. 6	2.66×10^{-2}	1322	5	7
	1 (point no. 3), Fig. 8	0.146	2648	22	370
	3 (points no. 1, 2, 3)	0.178	198	0	0.37
$\sigma = 0.5\,°C$	1 (point no. 1), Fig. 5	0.543	1438	3	1.3
	1 (point no. 2), Fig. 7	0.522	2705	11	25
	1 (point no. 3), Fig. 9	0.595	4493	30	575
	3 (points nos. 1–3)	0.548	1464	3	1.3

where a is the thermal diffusivity (taken at $T = 20\,°C$), Δt is the time step of the inverse problem (10 s here), and e is the distance between the sensor and the surface the unknown heat flux density is applied. The value of Δt_i allows to evaluate the level of ill-posedness of the inverse problem. In practice, Δt_i should be greater than 0.01 [20]. It is equal to 0.4, 0.016 and 0.005 when the sensor is located at point nos. 1, 2 and 3 respectively. The inverse problem with the sensor at point no. 1 is therefore "easy", while it becomes quite difficult with sensor at point no. 2 and clearly ill-posed when using sensor at point no. 3. Consequently, as the distance between the sensor and the unknown heat flux density increases, it is necessary to use a more important stabilization procedure to get a solution: the number ***nf*** of FTS needs to be increased in order to take into account heat diffusion effects (cf. Table 2). For example, when the sensor is located at point no. 2, some of the specific variations of the input signal are hardly perceptible on the temperature response, and when the sensor is located at point no. 3, they become invisible on the temperature response (cf. Fig. 3). Consequently, no FTS are needed with sensor no. 1 and "exact data" ($\boldsymbol{nf} = 0$), but 5 FTS are required with sensor no. 2 and 22 with sensor no. 3. In

Table 3
Inversion results for sensor at point no. 1 using RMs of order 1–5

Standard deviation of noise	RM's order n	σ_Y (°C)	σ_U ($W m^{-2}$)	Number ***nf*** of *Future Time Steps*	Order of magnitude of CPU time (s)
$\sigma = 0$ °C	1	5.87×10^{-15}	9034	0	0.21
	2	7.22×10^{-15}	630	0	0.26
	3	8.61×10^{-15}	433	0	0.28
	4	9.75×10^{-15}	195	0	0.37
	5	1.05×10^{-14}	159	0	0.63
$\sigma = 0.5$ °C	1	0.530	8707	3	0.64
	2	0.543	1552	3	0.8
	3	0.555	1401	3	0.93
	4	0.543	1438	3	1.3
	5	0.542	1445	3	2.6

this last case, values of ***nf*** in the range 0–21 have not led to a solution: the first solution has been obtained with ***nf*** = 22. Although FTS allow to diminish oscillations, important information is lost, especially the signal singularities and the sinusoid amplitude (cf. Figs. 4, 6 and 8). This is confirmed by the increase of σ_Y and σ_U (cf. Table 2). When the 3 sensors are used together instead of sensor no. 1 alone, the estimation is not improved: the values of σ_U are similar for both cases (cf. Table 2, and that is verified for exact and noised data). That is confirmed by the value of ***nf*** which is the same with 3 sensors and with sensor no. 1 alone (see Table 2). In addition, the inverse problem is already overdetermined as soon as ***nf*** > 0, even with a single sensor.

In the case of perturbed data, measurement errors are amplified through the inverse problem and oscillations appear in the estimated signal. Of course oscillations increase with the distance between the sensor and the unknown heat flux density because the inverse problem becomes more ill-posed (cf. Figs. 5, 7 and 9). This observation is confirmed by the increasing value of σ_U (cf. Table 2). As previously mentioned, the number ***nf*** of FTS is determined according to the *discrepancy principle* (Eq. (27)). Hence σ_Y values are about equal to the standard deviation of noise $\sigma = 0.5$ °C (cf. Table 2). In comparison with the case of "exact data", ***nf*** usually needs to be increased to obtain satisfying estimations, but with sensor no. 3 alone, values of ***nf*** in the range 0–29 have not led to a solution: the first solution has been obtained with ***nf*** = 30, corresponding to $\sigma_Y = 0.595$ °C ($> \sigma = 0.5$ °C).

Table 3 shows inversion results for sensor at point no. 1 when RMs of order 1–5 are used to perform the inversion. In the case of exact data, the more accurate is the RM (in terms of the discrepancy between its responses and DM's ones, cf. Part I of the paper [17]), the better is the heat flux density estimation. In the case of noised data ($\sigma = 0.5$ °C), the estimation obtained with RM of order 1 is not good while results for orders 2–5 are satisfying and of similar quality. This can be explained. The mean discrepancy $\boldsymbol{\sigma}_Y^{\mathrm{id}} = \sqrt{J_{\mathrm{red}}/(q(\mathrm{nt}+1))}$ between DM and RM of order 1 is 1.4 °C, which is higher than the standard deviation of noise 0.5 °C added to DM's outputs, hence the poor quality of RM of order 1 can be seen in inversion results. On the contrary, The mean discrepancy $\boldsymbol{\sigma}_Y^{\mathrm{id}}$ between DM and RMs of order 2–5 is lower than the level of noise 0.5 °C. The consequence is that the accuracy of these four RMs, increasing from 2 to 5, is no more relevant in that inversion case, and that the RM of order 2 gives an estimation nearly as good as the RM of order 5.

All the presented results tend to show the efficiency of the proposed inversion method and the robustness of the Reduced Model.

Note. As in many nonlinear problems, in some cases it has been necessary to introduce an under-relaxation method (Eq. (26)) in the algorithm described in Section 4, to ensure the stability of the iterative procedure at each time step. In the present study, relaxation has been used when a single sensor at point no. 2 or point no. 3 is used.

7. Conclusion

A method for solving nonlinear multidimensional transient Inverse Heat Conduction Problems using a Reduced Model (RM) is proposed in this numerical study.

The RM is identified through a specific procedure using optimization techniques. In comparison with a Detailed Model (DM) built with Finite Volumes Method, computing time for the direct problem resolution is drastically reduced without significant loss of accuracy.

A sequential algorithm is described, which allows for the estimation of a time-varying boundary condition or internal heat source. The *Function specification Method* permits to use additional information at *Future Time Steps*, in order to take into account lagging and damping effects of heat diffusion and improve the quality of estimations.

In this study and for the presented example, whereas it has not been possible to obtain stable solutions for the inverse problem with the DM associated to the proposed inversion algorithm using a simple Euler implicit scheme for time integration, the same simple algorithm has given satisfaction with RM, tending to prove that RMs can be used with rather coarse inversion algorithms. It should be noted that RM small size allows very fast computations and authorises a non prohibitive iterative treatment of nonlinearities.

A transient 3D example with thermal conductivity linearly dependant on temperature illustrates the method. A time-varying heat flux density is estimated from the knowledge of simulated temperature measurements inside the domain. Of course, the quality of the estimation depends on sensors location, but it has been shown that with a single sensor far from the heated boundary, it is possible to obtain an estimation of the unknown boundary condition, even in the presence of measurement errors.

In further studies, experimental data will be used, either for the RM identification and for the inverse problem resolution.

Among further developments, let us mention the extension to the more general case of both thermal conductivity and thermal capacity varying with temperature, as well as problems involving more than one independent time-varying unknown. The actual limitations are linked to the reduction method, which is at this time under improvement.

References

[1] J.V. Beck, B. Blackwell, C.R. St Clair, Inverse Heat Conduction: Ill-posed Problems, John Wiley, New York, 1985.

[2] A.N. Tikhonov, V.Y. Arsenin, Solutions of Ill-Posed Problems, V.H. Winston, Washington, DC, 1977.

[3] O.M. Alifanov, Inverse Heat Transfer Problems, Springer-Verlag, New York, 1994.

[4] J.R. Shenefelt, R. Luck, R.P. Taylor, J.T. Berry, Solution to inverse heat conduction problems employing singular value decomposition and model-reduction, Int. J. Heat Mass Transfer 45 (1) (2002) 67–74.

[5] Y. Jarny, M.N. Ozisik, J.P. Bardon, A general optimization method using adjoint equation for solving multidimensional inverse heat conduction, Int. J. Heat Mass Transfer 34 (11) (1991) 2911–2919.

[6] C.H. Huang, S.P. Wang, A three dimensional inverse heat conduction problem in estimating surface heat flux by conjugate gradient method, Int. J. Heat Mass Transfer 42 (18) (1999) 3387–3403.

[7] O.M. Alifanov, A.V. Nenarokomov, Three-dimensional boundary inverse heat conduction problem for regular coordinate systems, Inverse Problems in Engineering 7 (4) (1999) 335–362.

[8] J.V. Beck, Nonlinear estimation applied to the nonlinear inverse heat conduction problem, Int. J. Heat Mass Transfer 13 (4) (1970) 703–716.

[9] J.V. Beck, B. Litkouhi, C.RS.t. Clair, Efficient sequential solution of the nonlinear inverse heat conduction problem, Numer. Heat Transfer 5 (1982) 275–286.

[10] A.M. Osman, K.J. Dowding, J.V. Beck, Numerical solution of the general two-dimensional inverse heat conduction problem, Trans. ASME 119 (1997) 38–45.

[11] R. Pasquetti, C. Le Niliot, Boundary element approach for inverse heat conduction problems: application to a bidimensional transient numerical experiment, Numer. Heat Transfer B 20 (1991) 169–189.

[12] E. Videcoq, D. Petit, Model reduction for the resolution of multidimensional inverse heat conduction problems, Int. J. Heat Mass Transfer 44 (10) (2001) 1899–1911.

[13] M. Girault, D. Petit, E. Videcoq, The use of model reduction and function decomposition for identifying boundary conditions of a linear thermal system, Inverse Problems Eng. 11 (5) (2003) 425–455.

[14] H.M. Park, O.Y. Chung, J.H. Lee, On the solution of inverse heat transfer problem using the Karhunen-Loève–Galerkin method, Int. J. Heat Mass Transfer 42 (1) (1999) 127–142.

[15] H.M. Park, W.S. Jung, The Karhunen-Loève–Galerkin method for the inverse natural convection problems, Int. J. Heat Mass Transfer 44 (1) (2001) 155–167.

[16] A.J. Newman, Model reduction via the Karhunen-Loève expansion, Part I: an exposition, Technical Research Report of the Institute for Systems Research, University of Maryland, 1996. <http://techreports.isr.umd.edu/TechReports/ISR/1996/TR_96-32/TR_96-32.phtml>.

[17] M. Girault, D. Petit, Identification methods in nonlinear heat conduction, Part I: model reduction, Int. J. Heat Mass Transfer, submitted for publication.

[18] D. Petit, R. Hachette, D. Veyret, A modal identification method to reduce a high order model: application to heat conduction modelling, International Journal of Modelling and Simulation 17 (3) (1997) 242–250.

[19] J.V. Beck, B. Blackwell, A. Haji-Sheikh, Comparison of some inverse heat conduction methods using experimental data, Int. J. Heat Mass Transfer 39 (17) (1996) 3649–3657.

[20] G. Blanc, M. Raynaud, T.H. Chau, A guide for the use of the function specification method for 2D inverse heat conduction problems, Rev. Générale de Thermique 37 (1) (1998) 17–30.